Published in final edited form as:
Ann Otol Rhinol Laryngol. 2009 February ; 118(2): 131–138.

Surgical Method to Create Vocal Fold Injuries in Mice

Masaru Yamashita, MD, PhD, **Diane M. Bless, PhD**, and **Nathan V. Welham, PhD**
Division of Otolaryngology - Head and Neck Surgery, Department of Surgery, University of Wisconsin School of Medicine and Public Health, Madison, WI.

Abstract

Objectives—The goal of this study was to develop a surgical methodol for the creation of vocal fold injuries in mice, as a precursor to the use of genetically engineered mouse models in the study of vocal fold wound healing and scar formation.

Method—Seven FVB strain mice were used in this study. A laryngoscope and three micro-instruments were designed and fabricated to facilitate endoscopic vocal fold visualization and the creation of vocal fold surgical injuries. Larynges were harvested 1 and 7 days following surgery, and vocal fold injury sites were evaluated by routine Hematoxylin and Eosin staining. Additional immunohistochemical analysis of collagen type I and elastin distribution in the lamina propria was performed for a non-injured control larynx.

Results—Endoscopic visualization and vocal fold stripping resulting in thyroarytenoid muscle exposure were successful in all animals. Histological and immunohistochemical analyses revealed a simple lamina propria structure with relatively even collagen type I and elastin distribution in the control vocal fold, obliteration of vocal fold mucosa 1 day following surgery, and complete reepithelialization by 7 days.

Conclusion—These results demonstrate the feasibility of creating reproducible vocal fold injuries via an endoscopic approach in mice. The observation that the mouse lamina propria may have a relatively simple histological structure indicates that additional characterization should be performed and caution used when translating findings between this and other model systems.

Keywords

Vocal fold injury; scarring; mouse endoscopic surgery; histology; immunohistochemistry

Introduction

Vocal fold scarring often results in a severe and intractable dysphonia. [1, 2] An understanding of the wound healing process culminating in vocal fold scar is emerging in the literature, however the clinical management of this condition remains challenging and without consensus. The majority of work addressing scar formation and treatment in the vocal fold has relied on animal models such as the dog, pig, rabbit and rat.[3–11] Each model has distinct advantages and disadvantages in terms of vocal fold ultrastructural similarity to human, nature and extent of *in vivo* phonation, the availability of genome data and commercial antibodies, lifespan and metabolism, size and ease of handling, and cost.

Tateya et.al.[10] pioneered the use of a rat surgical model for studying vocal fold injury and scar formation. This model capitalized on a tri-layered lamina propria, ease of handling, relatively

Correspondence: Nathan V. Welham, PhD, K4/723 CSC, 600 Highland Avenue, Madison, WI 53792.
Presented at the 88th Annual Meeting of the American Broncho-Esophagological Association, Orlando, FL, May 2, 2008.

short life-span and fast scar maturation, and a strong scientific precedent in other organ systems. Although this model has afforded several scientific advantages unique to rodents, the rat is a challenging model for targeted genetic manipulation using knockout, knockdown, and knock-in technology. Knockout refers to the complete inactivation of a gene of interest, knockdown refers to a targeted reduction in gene expression, and knock-in refers to the targeted insertion of a functional cDNA sequence at a locus of interest. A select number of knockout rat models have been generated via induced mutagenesis followed by progeny screening;[12] however, in contrast, thousands of knockout, knockdown and knock-in mice models have been developed for a wide array of genes by targeted vector insertion and selection in embryonic stem cells, followed by cell delivery to mouse blastocysts.[13, 14] These genetically engineered animals have proven powerful tools in the study of individual gene function in development and disease.

The establishment of a mouse model of vocal fold injury and scar formation would facilitate the direct application of knockout, knockdown and knock-in technology to the study of this challenging condition. The primary barrier to the use of mice for this purpose is technical. Adult mice are less than 10% of the weight of their adult rat counterparts and the small size of the mouse larynx has previously restricted its use to non-surgical studies.[15–17] The purpose of this study was to overcome this challenge and establish a robust surgical approach to vocal fold injury creation in the mouse. This was achieved by surgical experimentation and the fabrication of several new micro-instruments. We evaluated surgical outcomes using routine histological preparation.

Materials and Methods

Seven male FVB strain mice (25.7 g ± 1.4 g) (Harlan Sprague Dawley, Indianapolis, IN) were used in this study. Six animals underwent vocal fold surgery and had tissue harvested at either 1 or 7 days post-surgery (N=3 per group). One animal was retained as a non-surgical control.

Anesthesia

Mice were anesthetized using isoflurane (2–3 % delivered at 0.8–1.5 L/min) followed by intraperitoneal (IP) injection of ketamine hydrochloride (50 mg/kg, Ketaject, Phoenix Pharmaceutical, St. Joseph, MO) and xylazine hydrochloride (4 mg/kg, Xyla-ject, Phoenix Pharmaceutical, St. Joseph, MO). Atropine sulfate (0.05 mg/ kg, Phoenix Pharmaceutical, St. Joseph, MO) was delivered IP to reduce production of saliva or sputum. Xylazine hydrochloride was employed as a topical anesthetic in the larynx and hypopharynx.

Laryngoscope

A custom designed laryngoscope was constructed of 1-mm-diameter stainless steel wire (Figure 1) to facilitate endoscopic visualization of the larynx. The anesthetized animals were placed in a supine position (Figure 2-A) and the laryngoscope positioned to provide an endoscopic surgical approach (Figure 2-B).

Endoscope and monitoring system

Surgical images were monitored using a 1.9-mm-diameter 25° endoscope (Richard Wolf, Vernon Hills, IL), CCD unit (596T, Stryker, San Jose, CA), light source (Q-5000, Stryker, San Jose, CA), monitor (PVN-1343MD, Sony, Tokyo, Japan), and digital hard disk video recorder (GZ-MG555U, Victor Company of Japan, Kanagawa, Japan) (Figure 3).

Surgical instrumentation and procedures

Three custom surgical instruments (needle, fork, and hook) were fabricated from commercial materials and used to induce vocal fold injuries. The needle instrument was based on a modified

25-gauge spinal needle (Sherwood Medical, St. Louis, MO). This needle contains a 0.2-mm-diameter thin inner wire, which was advanced 3 mm from the needle tip and fixed using solder. The wire tip was then bent approximately 15° to allow sufficient operating space in the laryngeal lumen when using the endoscope described above (Figure 4-A).

The fork instrument was fabricated using a 0.25-mm-diameter micro-fork (Electron Microscopy Sciences, Hatfield, PA). The micro-fork tip was cut, inserted and soldered to the tip of a 20-gauge spinal needle (Becton Dickinson, Franklin Lakes, NJ) (Figure 4-B).

The hook instrument was fabricated using 0.3-mm-diameter stainless steel wire, which was shaped and then soldered to a larger diameter stainless steel handle (Figure 4-C).

Unilateral vocal fold injuries were created as follows. First, the needle was inserted through the lateral aspect of the superior surface of the vocal fold (Figure 5-A) and then retracted in the medial direction to separate the mucosa from the underlying thyroarytenoid (TA) muscle (Figure 5-B). Care was taken to minimize disturbance of the TA muscle. Next, the fork was used to straddle the newly created mucosal bridge, and then rotated to strip the mucosa from its remaining TA muscle attachments (Figure 5-C). Finally, the hook was employed to expose any residual mucosal flaps and evaluate the degree of tissue injury. Surgery was completed once complete exposure of the TA muscle was obtained.

Tissue harvest and histological preparation

Mice were euthanized by CO_2 asphyxiation (3–4 L/min). The larynx was harvested en bloc under an operating microscope (Figure 6) and placed in phosphate buffered saline (PBS) containing 25 % sucrose for 8 hr at 4 °C. Next, the larynx was placed in a cryomold and embedded using optimal cutting temperature compound (Tissue-Tek, Sakura Finetechnical, Tokyo, Japan). Samples were frozen using acetone and dry ice.

Serial 7 μm axial cryosections were prepared using a cryostat (CM-1850, Leica, Wetzlar, Germany). Routine Hematoxylin and Eosin (H&E) staining was performed to confirm the vocal fold injury site. In addition, immunohistochemical (IHC) staining for the fibrous proteins collagen type I and elastin was performed for the control larynx. IHC was not performed for the injured samples as meaningful extracellular (ECM) remodeling was not anticipated during the first 7 days post-injury.

Fluorescent IHC was performed using the following standard protocol. Samples were fixed with 4% paraformaldehyde for 10 min at room temperature (RT) and treated with 0.5% triton X-100 (Sigma-Aldrich, St. Louis, MO) in blocking solution (1:10; BUF029, Serotec, Raleigh, NC) for 15 min at RT. Primary antibodies were applied for 1 hr at RT. Secondary antibodies were also applied for 1 hr at RT. 4`,6-diamidino-2-phenylindole dihydrochloride (2 mg/mL DAPI; MP Biomedicals, Santa Ana, CA) was applied for 20 min as a nuclear stain.

The primary antibodies used in this study were rabbit anti-collagen type I (1:50; ab34710, Abcam, Cambridge, MA) and goat anti-elastin (1:200; sc-17581, Santa Cruz Biotechnology, Santa Cruz, CA). The secondary antibodies used were anti-rabbit Alexa Fluor 594 (1:200; A-11012, Invitrogen, Carlsbad, CA) for collagen type I and anti-goat Alexa Fluor 488 (1:200; A-11078, Invitrogen, Carlsbad, CA) for elastin. Negative controls, for which samples were exposed to the secondary antibody in the absence of the primary antibody, revealed no immunostain.

Stained images were visualized and captured using a microscope with both conventional light and fluorescent capability (E600, Nikon, Tokyo, Japan) connected to a digital microscopy camera (DP70, Olympus, Tokyo, Japan).

Results

Vocal fold visualization was successfully achieved in all 7 mice. Figure 7 contains two representative images from an intact mouse larynx.

Unilateral vocal fold injuries were successfully created in the 6 mice that underwent surgery. One mouse developed post-operative stridor secondary to laryngeal edema which was successfully managed by delivery of 100 % O_2 at 3 L/min for approximately 30 minutes. Intubation was not attempted due to the risk of exacerbating the laryngeal edema.

Representative IHC data showing collagen type I and elastin distribution in the control larynx are presented in Figure 8 and Figure 9. Collagen type I was diffusely present throughout the entire lamina propria, and densely concentrated in the basement membrane region. Elastin immunostaining demonstrated sparse cellular and ECM distribution throughout the lamina propria, with greater abundance in the epithelium. The anti-elastin antibody employed in this study binds to both the precursor tropoelastin and mature elastin.

Figure 10-A illustrates an H&E stained section from the control mouse larynx. The lamina propria was characterized by a relatively simple structure. Figure 10-B illustrates an H&E stained section from a larynx harvested 1 day following surgery. The operated vocal fold was characterized by obliteration of the epithelial and subepithelial structures, a fibrin clot and lymphocyte infiltration. Sections from the other two larynges harvested 1 day following surgery also demonstrated these features.

Seven days following surgery, injured vocal folds from all 3 animals demonstrated complete reepithelialization. Two samples were characterized by a relatively sparse lamina propria structure in the injured vocal fold compared with the control vocal fold (Figure 10-C); whereas the third sample showed no difference between the injured and control vocal folds.

Discussion

The goal of this study was to develop a surgical methodology for the creation of vocal fold injuries in mice, as a precursor to the use of genetically engineered mouse models in the study of vocal fold wound healing and scar formation. A laryngoscope and three surgical instruments were designed and fabricated for this purpose. The needle instrument was designed to make a superior vocal fold incision without interference from the epiglottis or working endoscope. The fork instrument was designed to facilitate the removal of vocal fold mucosa given limited operating space in the laryngeal lumen. The hook instrument was designed to evaluate the extent of vocal fold injury following use of the needle and fork. Operating with the mouse in a supine position enabled us to manipulate all instruments with maximum accuracy and control. A lightweight CCD camera module and 25° endoscope were also critical to successful vocal fold visualization and surgical manipulation.

We utilized fluorescent IHC to evaluate collagen type I and elastin distribution in the uninjured mouse vocal fold, and routine H&E staining to evaluate the vocal fold injury site and reepithelialization in each experimental animal. Our initial experience processing laryngeal samples without sucrose treatment resulted in significant image artifact due to ice crystal formation in the TA muscle (data not shown). This artifact was not present in samples treated with 25 % sucrose for 8 hr. Our evaluation of the uninjured control mouse vocal fold revealed a relatively simple lamina propria structure with diffuse collagen type I and tropoelastin/elastin distribution. Both fibrous proteins demonstrated relatively even distribution as a function of lamina propria depth, with no apparent layer structure as has been reported in humans and other animal models.18 This finding is consistent with Abdelkafy et al.15 who reported fairly even collagen (Trichrome stain) and glycosaminoglycan (GAG, Alcian blue stain) distribution

throughout the vocal fold lamina propria of C57BL/6 strain mice, and identified decreased GAG abundance and increased collagen abundance in old compared with young mice. As noted earlier, we did not evaluate alteration in fibrous protein abundance or organization in the injured vocal folds in this study, as meaningful ECM remodeling was not anticipated during the first 7 days post-injury. Additional work is required to characterize this remodeling phase and eventual scar formation in the mouse model.

The data presented here demonstrate that the surgical removal of vocal fold mucosa is possible in the mouse. The three larynges harvested 1 day following surgery showed obliteration of the epithelium and lamina propria, deposition of a fibrin clot, and the infiltration of inflammatory cells. We observed reepithelialization of all injured vocal folds by 7 days post surgery, which is slightly faster than the 7–14 days reported by Tateya et al. in a Sprague Dawley rat model.[19] Two larynges out of three were characterized by relatively sparse lamina propria on the injured vocal fold side at 7 days. This finding could represent residual edema, immature crosslinking between regenerating fibers, or even an artifact in cryosectioning.

Conclusions

These results demonstrate the feasibility of creating reproducible vocal fold injuries via an endoscopic approach in mice. The availability of gene knockout, knockdown and knock-in models make the mouse an attractive candidate for studying individual targeted genes as they relate to vocal fold structure and function. The observation that the mouse lamina propria has a relatively simple histological structure indicates that additional characterization should be performed and caution used when translating findings between this and other model systems.

Acknowledgments

We acknowledge technical assistance and consultation provided by Ronald McCabe, B.S.E.E. and Kimberly Maurer, M.S., C.V.T..

This study was supported by grant R01 DC004428 from the National Institute on Deafness and Other Communication Disorders. This study was performed in accordance with the PHS Policy on Humane Care and Use of Laboratory Animals, and the Animal Welfare Act (7 U.S.C et seq.); the animal use protocol was approved by the Institutional Animal Care and Use Committee (IACUC) of the University of Wisconsin-Madison.

References

1. Hansen JK, Thibeault SL. Current understanding and review of the literature: Vocal fold scarring. J Voice 2006;20:110–120. [PubMed: 15964741]
2. Hirano S. Current treatment of vocal fold scarring. Curr Opin Otolaryngol Head Neck Surg 2005;13:143–147. [PubMed: 15908810]
3. Chan RW, Siegmund T. Vocal fold tissue failure: Preliminary data and constitutive modeling. J Biomech Eng 2004;126:466–474. [PubMed: 15543864]
4. Garrett CG, Coleman JR, Reinisch L. Comparative histology and vibration of the vocal folds: Implications for experimental studies in microlaryngeal surgery. Laryngoscope 2000;110:814–824. [PubMed: 10807360]
5. Hirano S, Bless DM, Rousseau B, Welham NV, Scheidt T, Ford CN. Fibronectin and adhesion molecules on canine scarred vocal folds. Laryngoscope 2003;113:966–972. [PubMed: 12782806]
6. Kriesel KJ, Thibeault SL, Chan RW, Suzuki T, VanGroll PJ, Bless DM, Ford CN. Treatment of vocal fold scarring: Rheological and histological measures of homologous collagen matrix. Ann Otol Rhinol Laryngol 2002;111:884–889. [PubMed: 12389855]
7. Rousseau B, Hirano S, Chan RW, Welham NV, Thibeault SL, Ford CN, Bless DM. Characterization of chronic vocal fold scarring in a rabbit model. J Voice 2004;18:116–124. [PubMed: 15070231]
8. Rousseau B, Hirano S, Scheidt TD, Welham NV, Thibeault SL, Chan RW, Bless DM. Characterization of vocal fold scarring in a canine model. Laryngoscope 2003;113:620–627. [PubMed: 12671417]

9. Rousseau B, Tateya I, Lim X, Muñoz del Río A, Bless DM. Investigation of anti-hyaluronidase treatment on vocal fold wound healing. J Voice 2006;20:443–451. [PubMed: 16243482]
10. Tateya T, Tateya I, Sohn JH, Bless DM. Histologic characterization of rat vocal fold scarring. Ann Otol Rhinol Laryngol 2005;114:183–191. [PubMed: 15825566]
11. Thibeault SL, Gray SD, Bless DM, Chan RW, Ford CN. Histologic and rheologic characterization of vocal fold scarring. J Voice 2002;16:96–104. [PubMed: 12002893]
12. Zan Y, Haag JD, Chen KS, Shepel LA, Wigington D, Wang YR, Hu R, Lopez-Guajardo CC, Brose HL, Porter KI, Leonard RA, Hitt AA, Schommer SL, Elegbede AF, Gould MN. Production of knockout rats using ENU mutagenesis and a yeast-based screening assay. Nat Biotechnol 2003;21:645–651. [PubMed: 12754522]
13. Capecchi MR. The new mouse genetics: altering the genome by gene targeting. Trends Genet 1989;5:70–76. [PubMed: 2660363]
14. Capecchi MR. Altering the genome by homologous recombination. Science 1989;244:1288–1292. [PubMed: 2660260]
15. Abdelkafy WM, Smith JQ, Henriquez OA, Golub JS, Xu J, Rojas M, Brigham KL, Johns MM. Age-related changes in the murine larynx: Initial validation of a mouse model. Ann Otol Rhinol Laryngol 2007;116:618–622. [PubMed: 17847730]
16. Renne RA, Gideon KM, Miller RA, Mellick PW, Grumbein SL. Histologic methods and interspecies variations in the laryngeal histology of F344/N rats and B6C3F1 mice. Toxicol Pathol 1992;20:44–51. [PubMed: 1411130]
17. Nishio T, Bando H, Bamba H, Hisa Y, Okamura H. Circadian gene expression in the murine larynx. Auris Nasus Larynx. (in press).
18. Kurita, S.; Nagata, K.; Hirano, M. A comparative study of the layer structure of the vocal fold. In: Bless, DM.; Abbs, JH., editors. Vocal fold physiology: Contemporary research and clinical issues. San Diego: College-Hill Press; 1983. p. 3-21.
19. Tateya T, Tateya I, Sohn JH, Bless DM. Histological study of acute vocal fold injury in a rat model. Ann Otol Rhinol Laryngol 2006;115:285–292. [PubMed: 16676825]

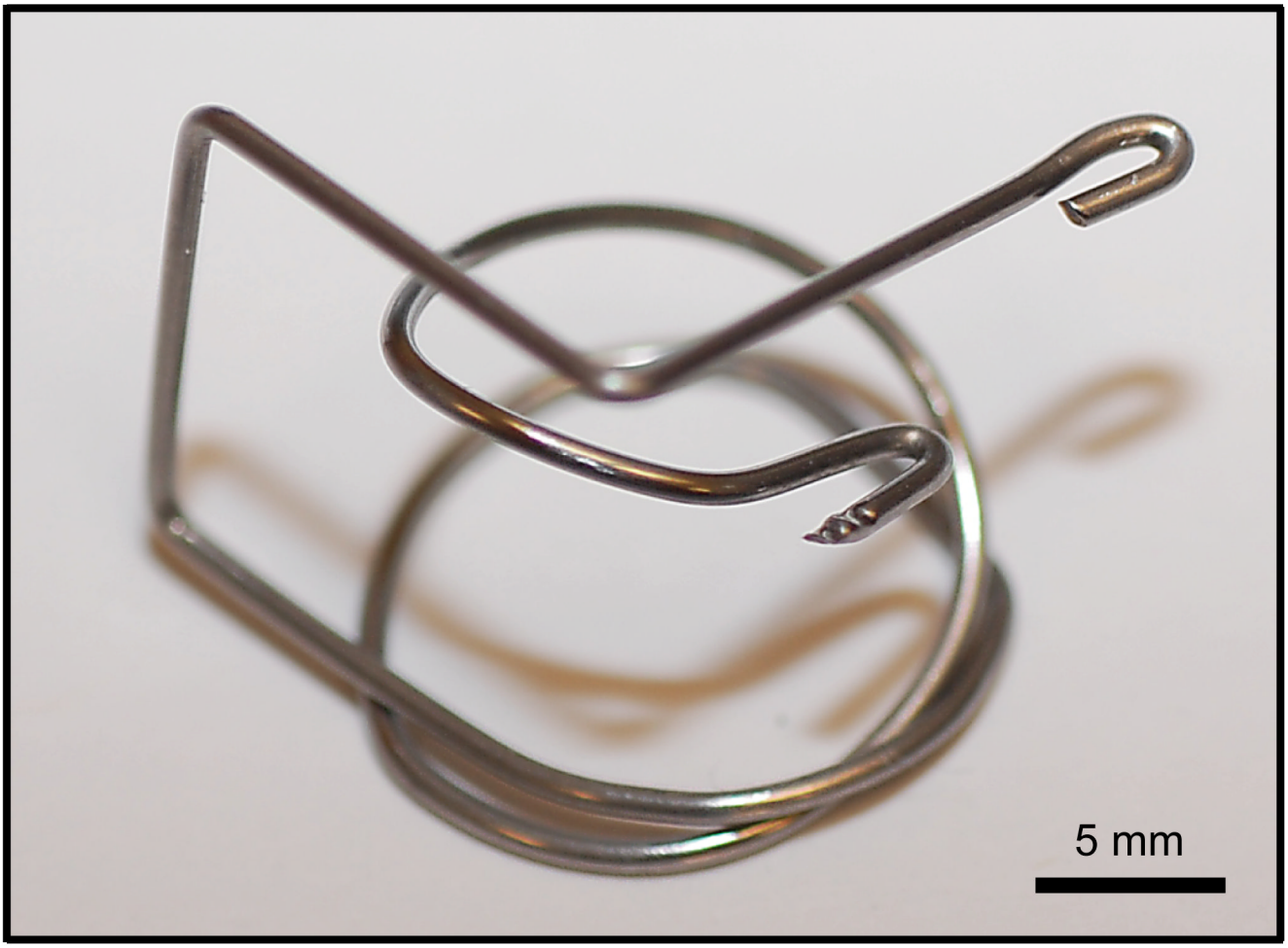

Figure 1.
Custom made mouse laryngoscope fabricated from 1-mm-diameter stainless steel wire.

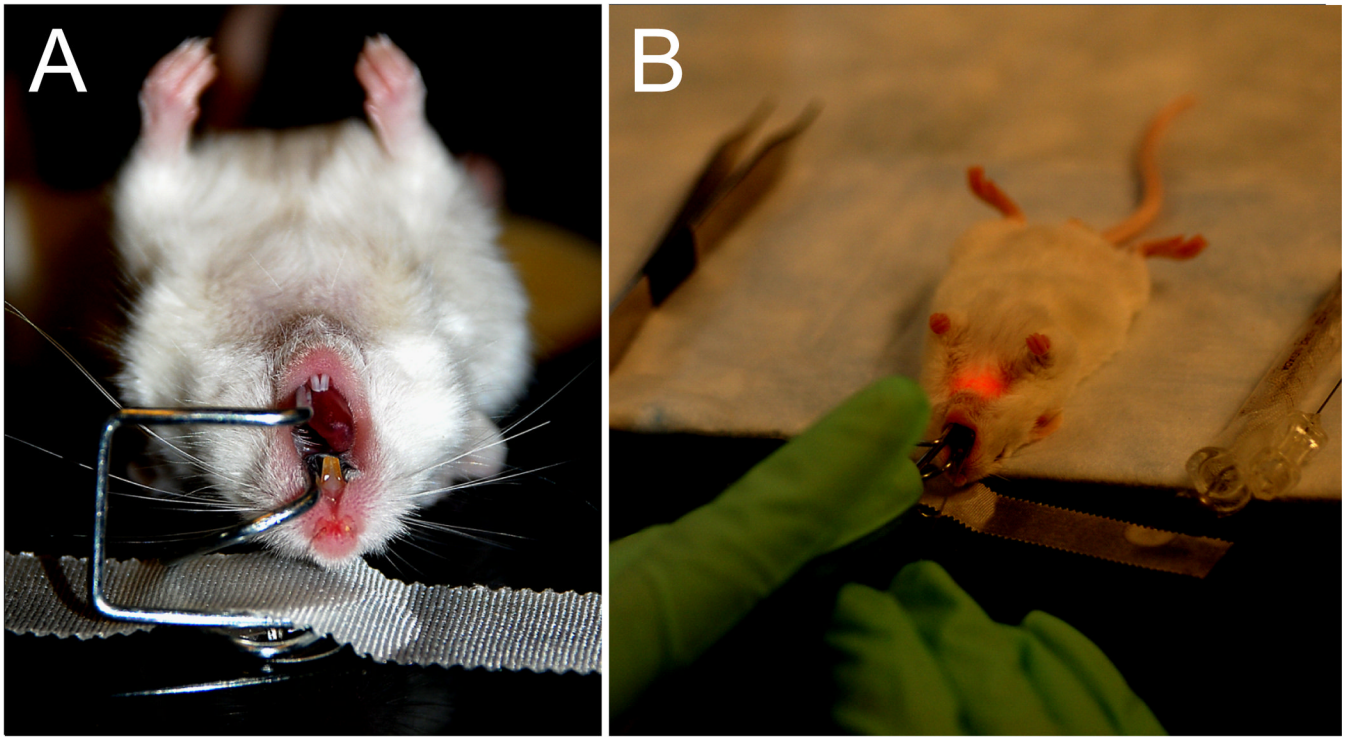

Figure 2.
A: Anesthetized FVB mouse in supine orientation with the laryngoscope inserted. B: Surgical procedure performed transorally under endoscopic guidance.

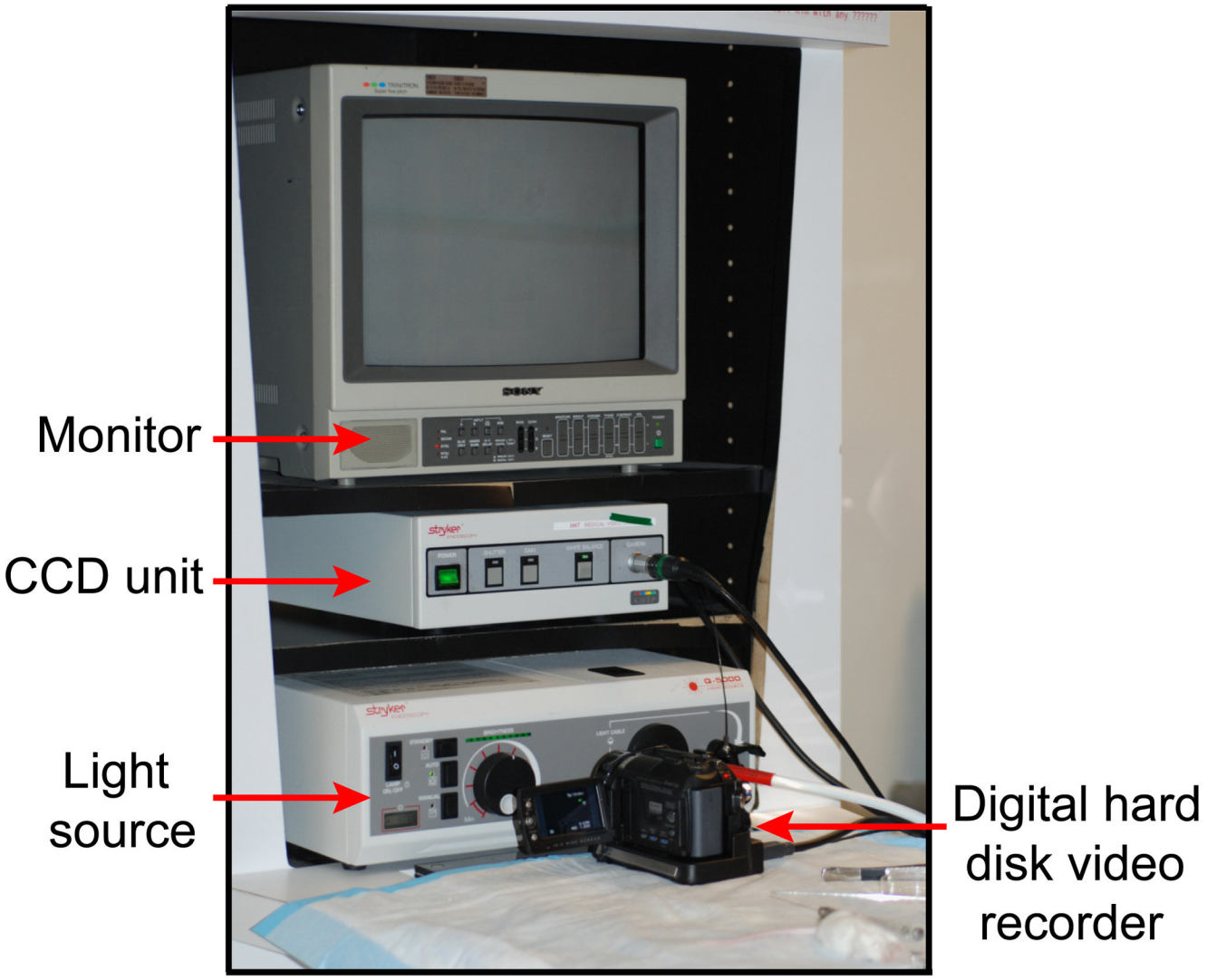

Figure 3.
Surgical monitoring and recording system employed in this study.

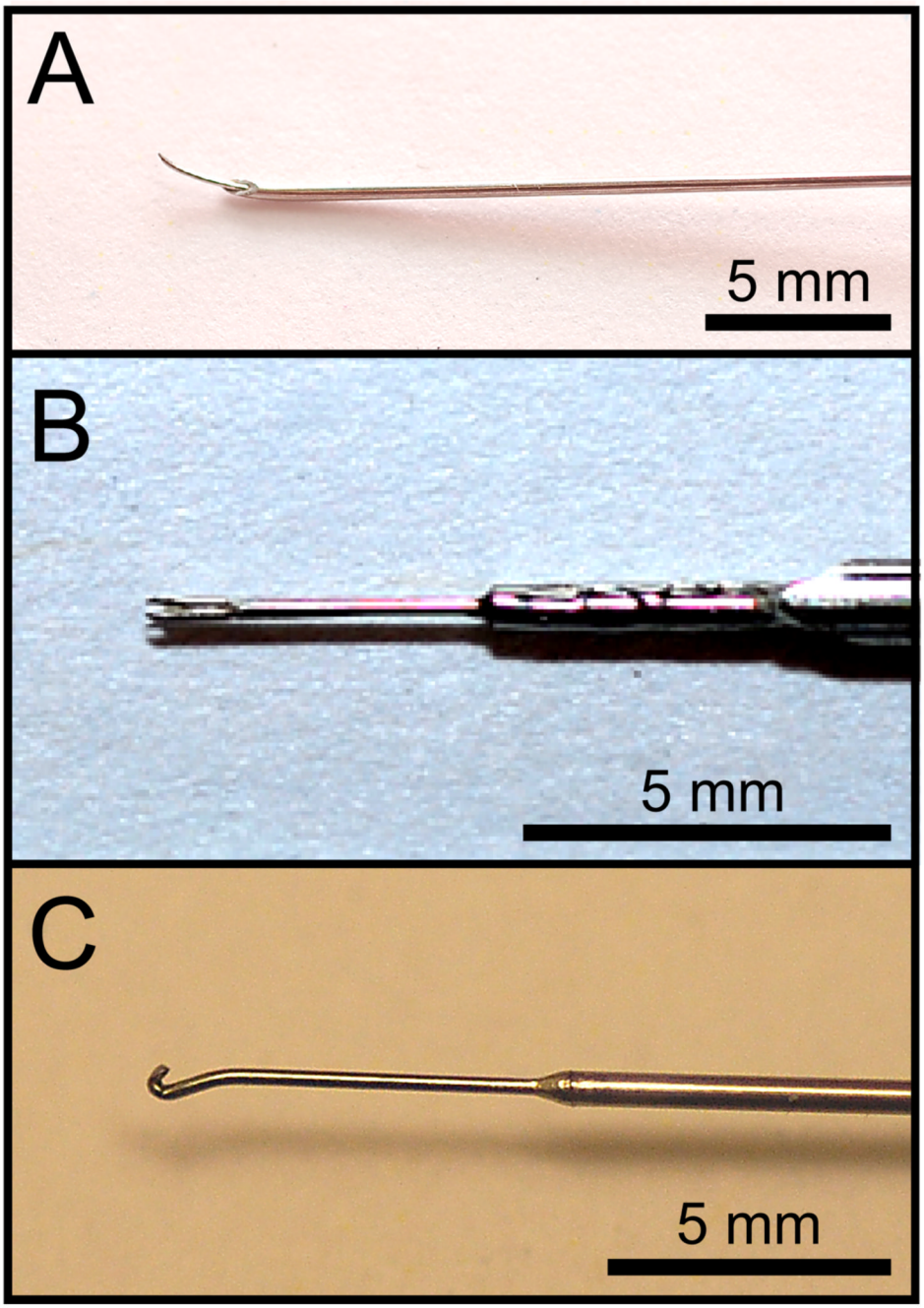

Figure 4.
Surgical micro-instruments designed and fabricated for this study. A: Needle instrument. B: Fork instrument. C: Hook instrument.

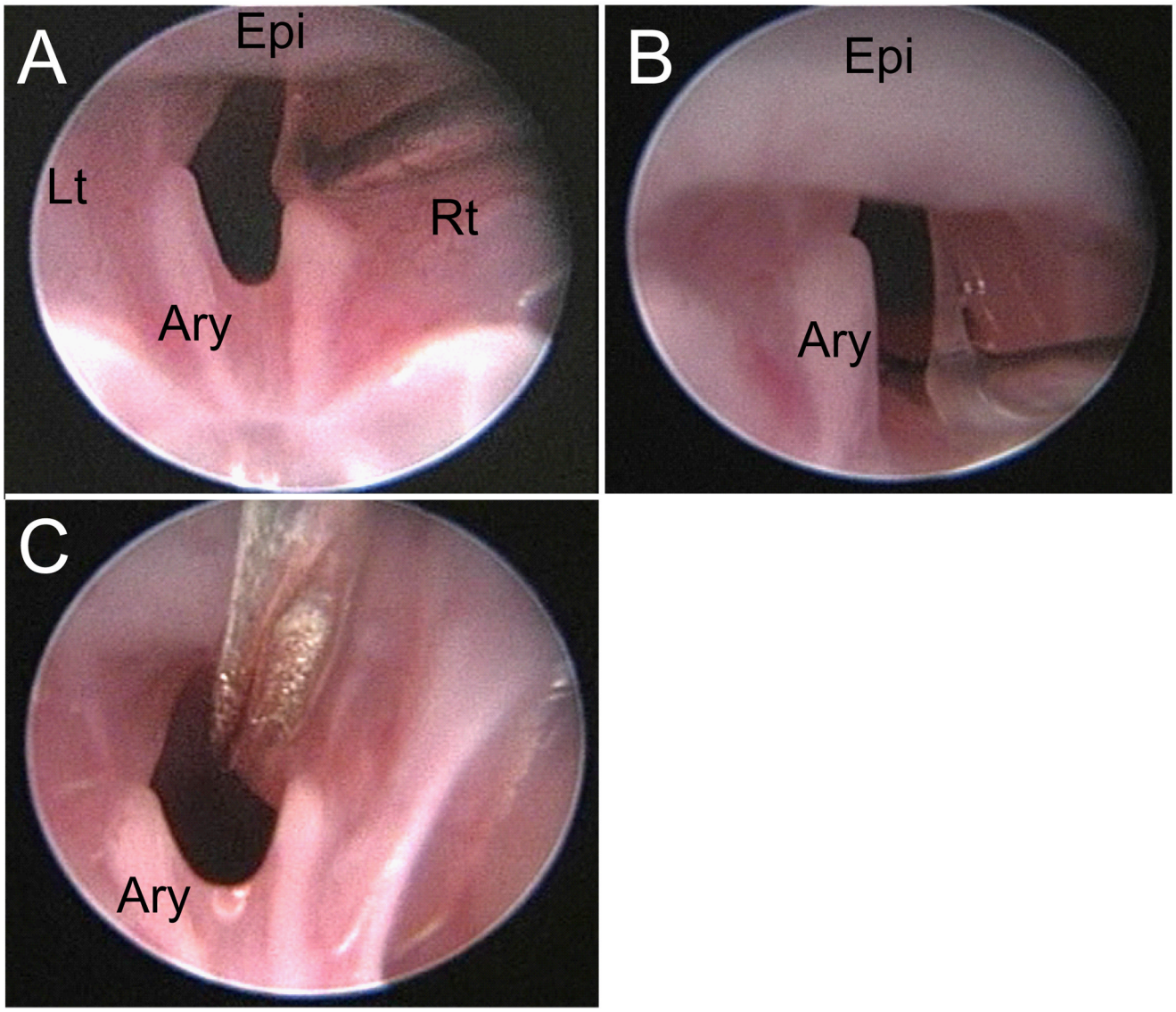

Figure 5.
Endoscopic images collected during the vocal fold injury procedure. A: Needle insertion at the lateral aspect of the superior surface of the right vocal fold. B: Retraction of the vocal fold mucosa in the medial direction. C: Placement of the fork instrument prior to rotation and mucosal stripping. Epi: epiglottis; Ary: left arytenoid; Rt: right; Lt: left.

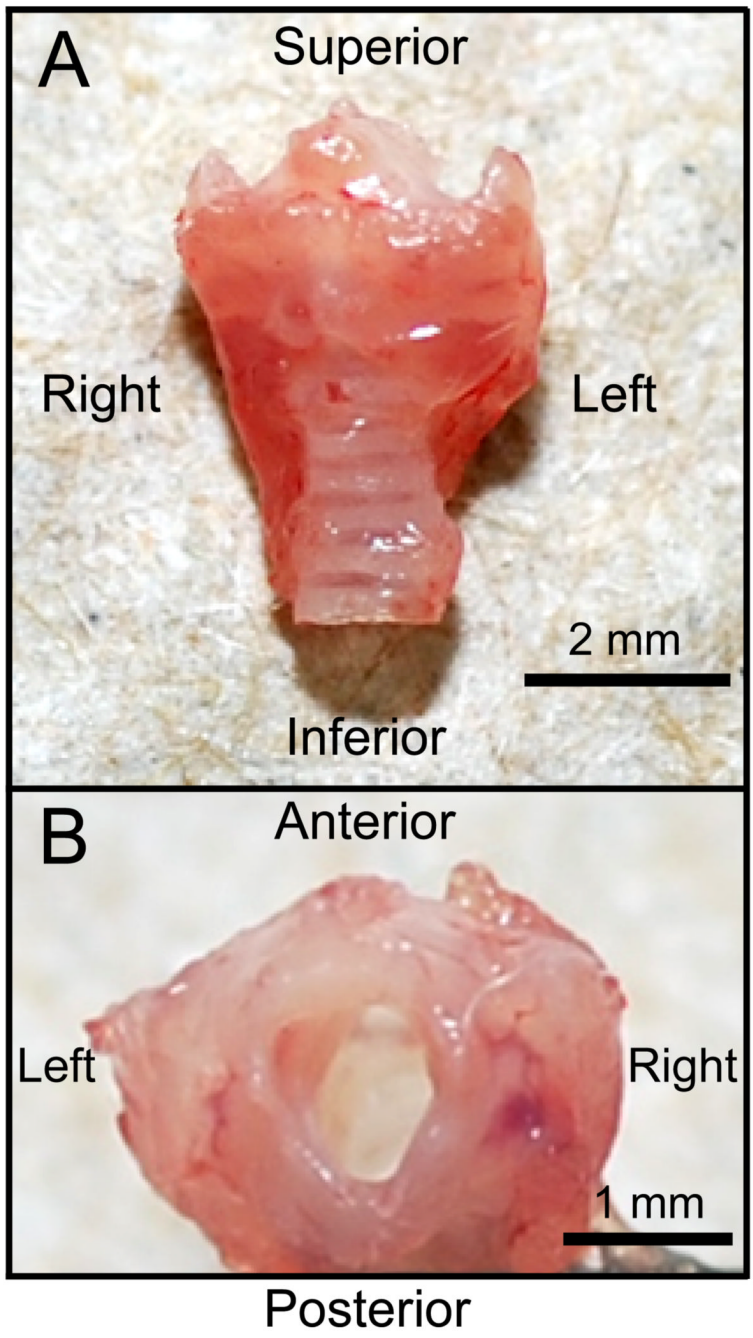

Figure 6.
Anterior (A) and superior (B) macroscopic views of a harvested mouse larynx.

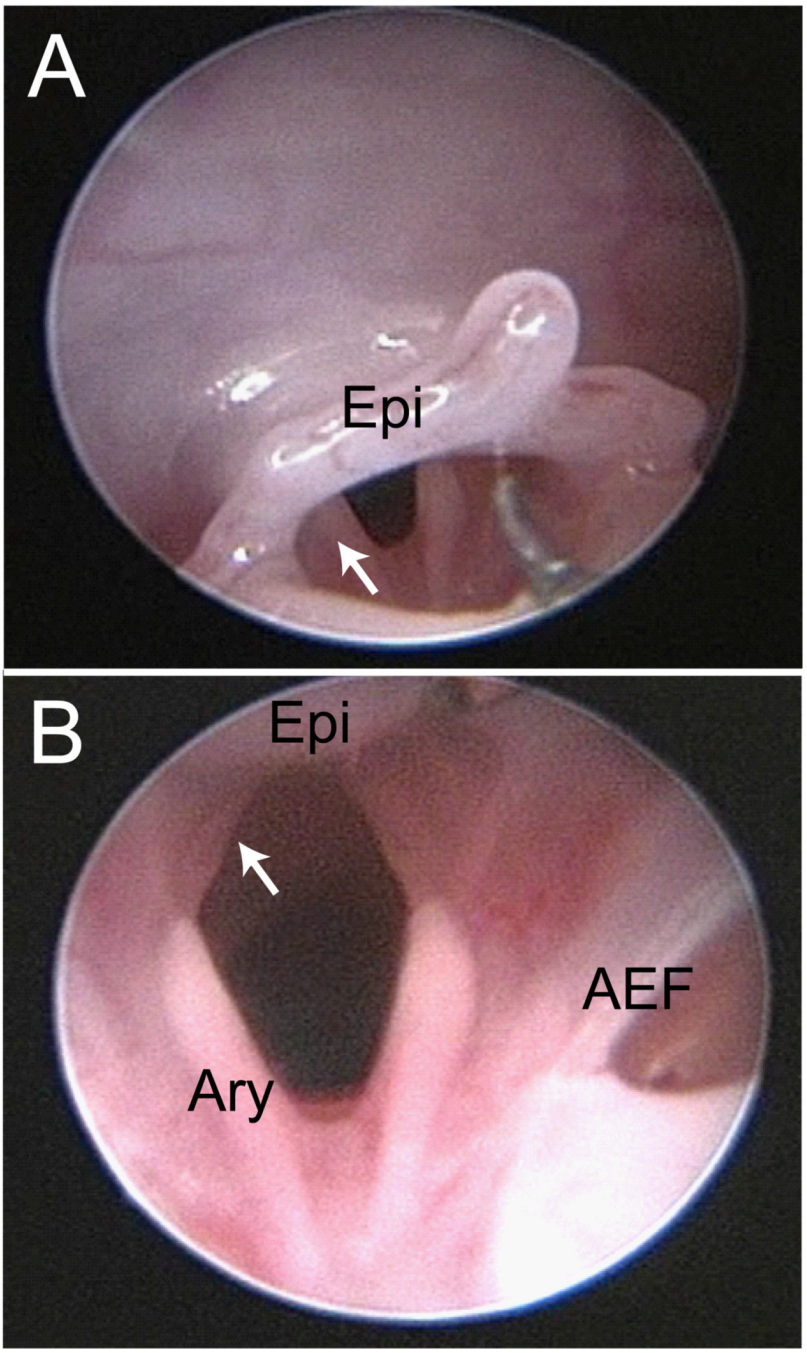

Figure 7.
Endoscopic images of an uninjured mouse larynx. A: View from the oropharynx. The white arrow indicates the left arytenoid cartilage. B: View from the supraglottis. The white arrow indicates the left membranous vocal fold. AEF: right aryepiglottic fold; Ary: left arytenoid cartilage; Epi: epiglottis.

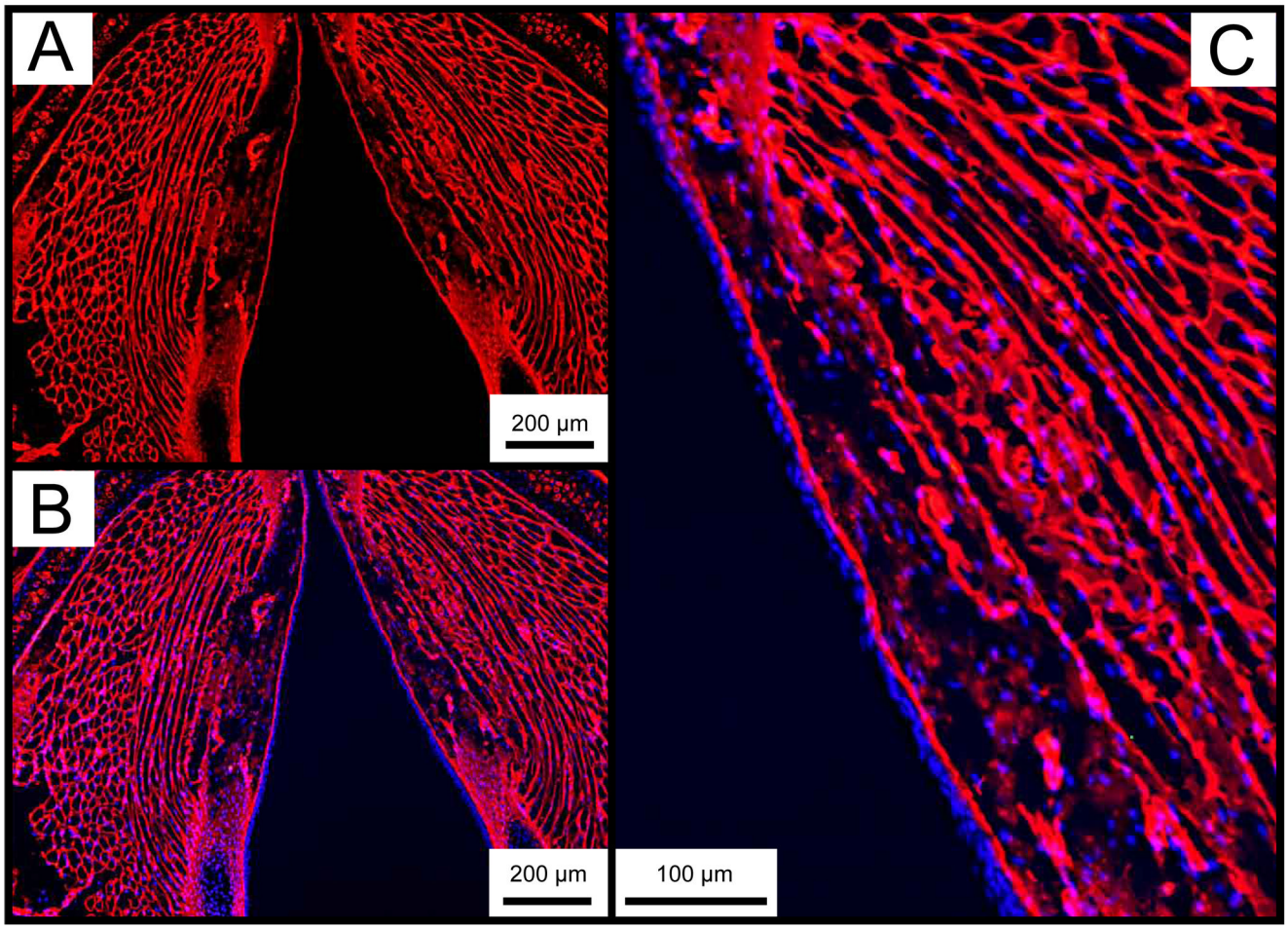

Figure 8.
Representative whole mount axial laryngeal sections from an uninjured control mouse, immunostained for collagen type I. A: Collagen type I is stained red (Alexa Fluor 594). B: Merged image of A and the same section stained with DAPI. Cell nuclei are stained blue. C: Magnified image of B showing the right vocal fold with diffuse collagen type I distribution throughout the lamina propria.

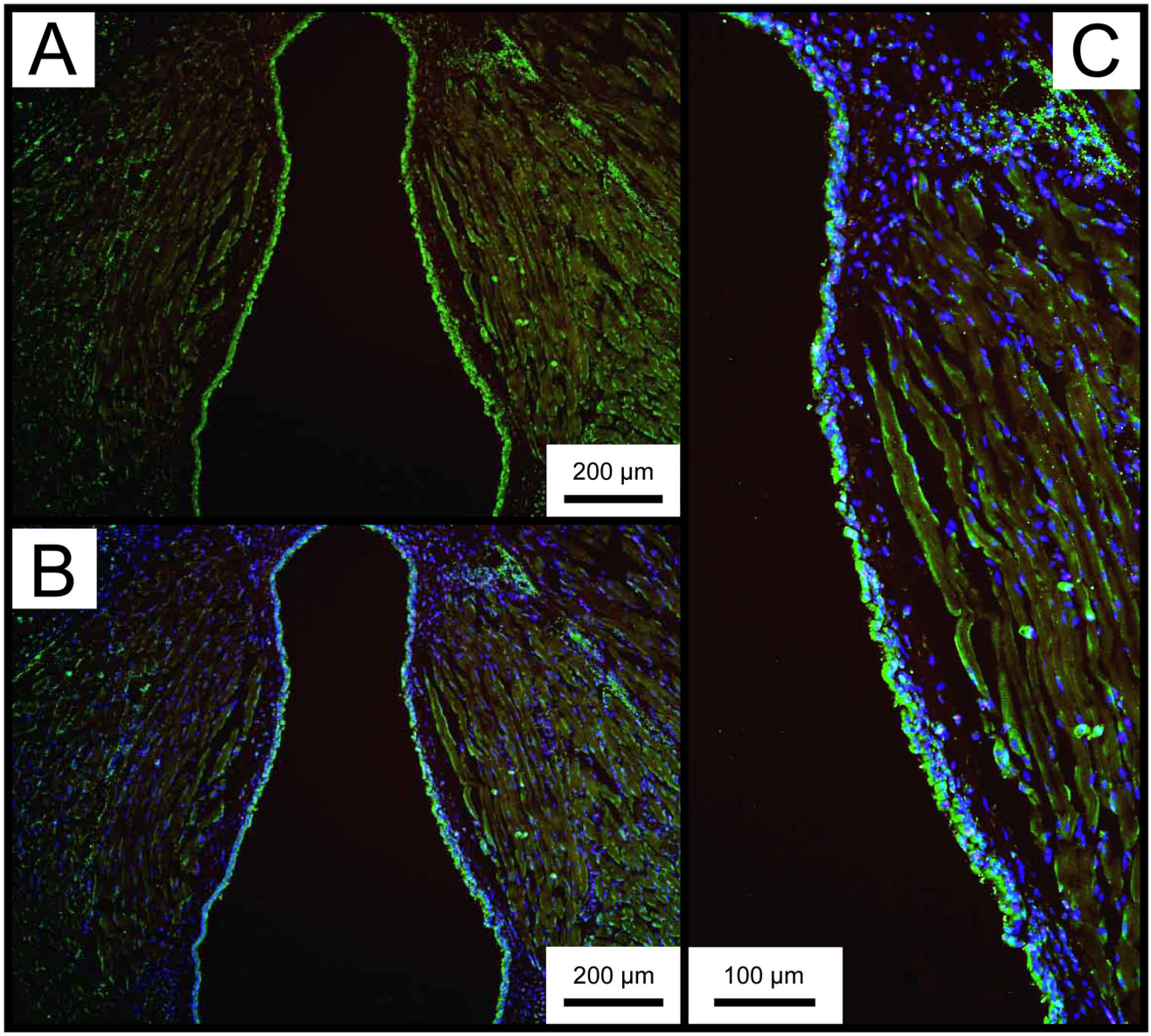

Figure 9.
Representative whole mount axial laryngeal sections from an uninjured control mouse, immunostained for tropoelastin/elastin. A: Tropoelastin/elastin is stained green (Alexa Fluor 488). B: Merged image of A and the same section stained with DAPI. Cell nuclei are stained blue. C: Magnified image of B showing the right vocal fold with sparse tropoelastin/elastin distribution throughout the lamina propria.

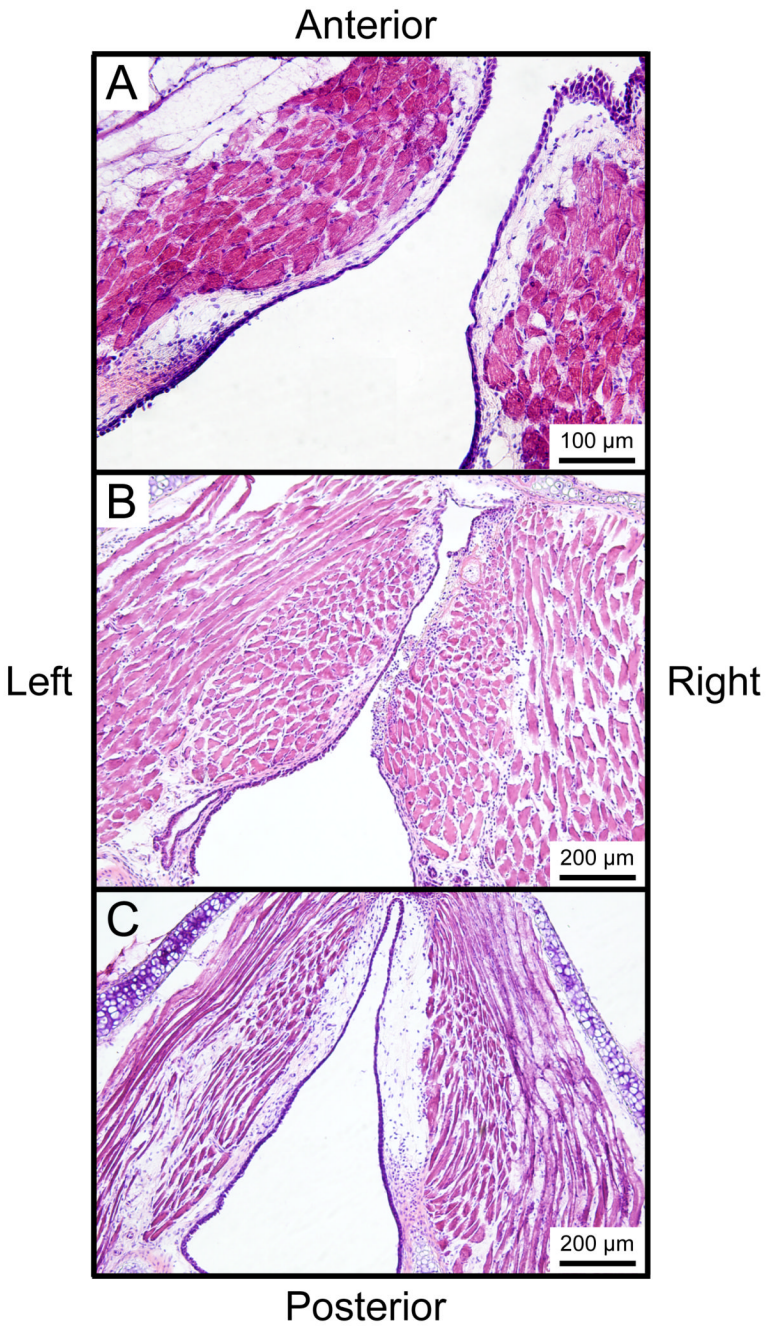

Figure 10.
Whole mount axial laryngeal sections stained with Hematoxylin & Eosin. A: Uninjured control vocal folds. B: One day following right vocal fold injury showing obliteration of the epithelium and lamina propria, deposition of fibrin clot, and infiltration of inflammatory cells. C: Seven days following right vocal fold injury showing complete reepithelialization and a relatively sparse lamina propria structure.